Design of an AASS with Angular Selectivity and Switchable Transmission States

Jiaying Li*, Xiao Li
School of Information and Navigation, Air Force Engineering University, Xi'an, Shaanxi, China
**Corresponding Author*

Abstract: This paper proposes an active angle-selective surface (AASS) with angular selectivity and adjustable transmission states. The suggested structure consists of two angle-selective surface (ASS) layers with the same configuration and a transmission-reflection switchable active frequency selective surface (AFSS) layer. The upper ASS layers are employed to obtain angular selectivity by forming a transmission window at a specific incident angle, while effectively reflecting electromagnetic waves at other angles. The lower AFSS layer utilizes PIN diodes to enable the variation of electromagnetic response. Numerical simulation and analysis indicate that, at the operating frequency of 11.75 GHz, the proposed system exhibits notable angular selectivity under TM-polarized incidence, guaranteeing high transmission only at an incident angle of 60° and maintaining strong reflection for other angles. Additionally, the transmission and shielding states can be rapidly changed by adjusting the working conditions of the AFSS when the incident angle is 60°, thus providing dual control over angular selectivity and electromagnetic response. This proposed design provides a promising solution for spatial filtering and directional communication in complex electromagnetic environments, with good potential applications in practical engineering.

Keywords: Active Frequency Selective Surface (AFSS); Angle-Selective Surface (ASS); Reconfigurable Structures; State Switching; Equivalent Circuit Model (ECM).

1. Introduction

Frequency selective surfaces (FSSs) are two-dimensional periodic electromagnetic structures that regulate how incident electromagnetic waves are transmitted or reflected [1-3]. Owing to this field-control capability, they have been used in radar stealth, radomes, electromagnetic shielding, spatial filtering, and related applications [4-7]. As electromagnetic operating environments become more complex, however, conventional FSSs that depend mainly on frequency selectivity expose a clear limitation: they do not by themselves address angular selectivity, polarization control, or dynamic reconfigurability [8-10]. This gap has motivated renewed interest in FSS-based structures that combine angular selectivity with reconfigurable electromagnetic responses.

Angle-selective surfaces (ASSs) extend the filtering mechanism from the frequency domain to the spatial domain. In a typical design, waves incident within a prescribed angular range are allowed to pass, whereas waves arriving from other directions are reflected or suppressed, so the propagation direction can be controlled more selectively [11,12]. Reported implementations include schemes based on planar optics, the Brewster angle principle, angularly sensitive FSS configurations, and anisotropic unit cells [13-15]. For example, Mao et al. proposed a broadband dual-polarized ASS based on multilayer FSSs, obtaining high transmission at normal incidence and strong reflection under oblique incidence [16]. Hong et al. introduced a longitudinal component in a three-dimensional ASS to tune the electromagnetic response for different incidence angles [17]. Zhang et al. further reported a via-free two-dimensional ASS that combines a grid structure with crossed dipole elements, permitting transmission below 20 degrees while reflecting waves above 47 degrees [18]. These studies demonstrate the feasibility of angular filtering, but most reported ASSs remain passive; after fabrication, their electromagnetic response is essentially fixed, which limits their adaptability in changing electromagnetic environments.

Active frequency selective surfaces (AFSSs) address this lack of tunability by loading the surface with controllable elements, such as PIN

diodes, varactor diodes, or MEMS devices. With these components, an AFSS can switch between operating states or adjust its operating band [19,20]. Li et al. proposed a compact dual-layer AFSS derived from filter-circuit topology, realizing independent switching between passband and stopband responses while maintaining angular stability within 45 degrees [21]. Wang et al. presented an active second-order FSS composed of three symmetric layers, which achieved switching between broadband transmission and broadband shielding for incidence angles up to 60 degrees [22]. Although these results indicate the value of AFSSs for reconfigurable electromagnetic devices, much of the existing work still concentrates on frequency tuning or state switching. Selective manipulation in the angular domain has received comparatively less attention.

Therefore, to address the challenge that interference signals and desired signals often overlap in the frequency domain and cannot be effectively separated using conventional frequency-selective approaches, and to enhance the adaptive control capability of systems in complex electromagnetic environments, integrating angular selectivity with active reconfigurability has become an important direction for achieving dynamic electromagnetic manipulation in the spatial domain. However, the incorporation of angular selectivity and active tuning mechanisms often introduces mutual coupling effects, which increase design complexity and make it difficult to simultaneously achieve optimal angular selectivity and reconfigurable performance.

To address the aforementioned challenges, this paper proposes a state-switchable angularly selective active angle-selective surface (AASS). The proposed structure consists of two cascaded ASS layers with identical topology and one AFSS layer, where the upper two layers are designed to achieve angular selectivity, and the bottom layer enables dynamic switching between transmission and reflection states. By carefully optimizing the structural parameters and interlayer coupling, the proposed design achieves high transmission only for TM-polarized waves at an incident angle of 60° at 11.75 GHz, while exhibiting strong reflection under all other incidence conditions. Furthermore, under the 60° incidence condition, the transmission and shielding states can be flexibly switched by controlling the operating states of the AFSS, thereby enabling simultaneous control over angular selectivity and electromagnetic response.

2. Structure Design and Theoretical Analysis

To simultaneously achieve angular selectivity and state switching, the ASS and AFSS are cascaded in a multilayer configuration. As illustrated in Figure 1, the upper ASS layers are responsible for angular filtering, while the lower AFSS layer enables dynamic state switching. Here, denotes the effective electrical length of the transmission line. Accordingly, the proposed structure can be modeled as a multilayer impedance network composed of cascaded ASS and AFSS layers. For an incident electromagnetic wave, each layer can be equivalently represented by a surface impedance that depends on both frequency and incident angle. The dielectric substrates and air spacings between adjacent layers can be modeled as transmission line sections. Therefore, the overall structure can be rigorously analyzed using the transmission matrix method.

$$\begin{bmatrix} A & B \\ C & D \end{bmatrix} = A_{ASS} A_{air} A_{AFSS} \tag{1}$$

From this model, the transmission and reflection coefficients of the equivalent circuit can be obtained,

$$\begin{aligned} S_{21} &= \frac{2}{A + B/Z_0 + CZ_0 + D} \\ S_{11} &= \frac{A + B/Z_0 - CZ_0 - D}{A + B/Z_0 + CZ_0 + D} \end{aligned} \tag{2}$$

where Z_0 denotes the intrinsic impedance of free space.

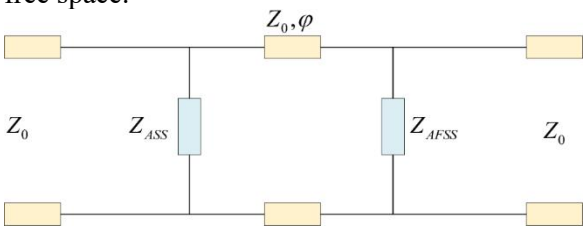

Figure 1. Equivalent Circuit Model of the Combined Structure of ASS and AFSS

For the ASS design, a double-layer FSS configuration is adopted. The equivalent circuit model (ECM) of the double-layer ASS is illustrated in Figure 2, where h represents the air thickness between the two FSS layers. Due to the presence of an air spacing between the two FSS layers, a Fabry–Pérot-like cavity resonance is formed. When the resonance condition is satisfied (3), a strong standing-wave field is established between the two FSS layers [23].

$$2\beta h + \varphi_r = 2\pi n \quad (3)$$

where h denotes the thickness of the air layer, β is the propagation constant, φ_r represents the reflection phase, and n is an integer.

Under this condition, the transmitted waves undergo constructive interference and continue to propagate, resulting in a resonance peak that varies significantly with the incident angle. Therefore, employing a double-layer FSS for ASS design enhances angular sensitivity. In addition, interlayer coupling introduces extra phase delay, such that constructive interference is satisfied only at specific incident angles, thereby further suppressing transmission at undesired angles.

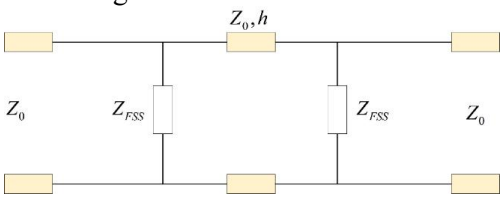

Figure 2. Equivalent Circuit Model of the Double-Layer ASS

Through proper design of the periodic unit cell, impedance matching between the incident electromagnetic wave and the ASS can be achieved at a specific incident angle, thereby forming a transmission passband. When the incident angle deviates from the designed value, the matching condition is disrupted due to the angle-dependent variation of Z_{ASS}, resulting in impedance mismatch and consequently strong reflection.

For the AFSS design, PIN diodes are incorporated into a bandpass FSS to enable reconfigurability. The corresponding ECM is shown in Figure 3, where the PIN diode is connected in parallel with the capacitor C. When the diode is in the ON state, it can be modeled as a series combination of a parasitic resistance and inductance. Under this condition, the resonant behavior shifts to a stopband response. When the diode is in the OFF state, it is equivalent to a capacitance, and the structure exhibits a passband resonance. In this way, dynamic switching between transmission and reflection can be achieved. Furthermore, by properly tuning the structure such that the passband resonance of the AFSS coincides with the transmission band of the ASS, and by optimizing the spacing between the two layers to mitigate mutual coupling effects, both angular selectivity and state-switching functionality can be simultaneously realized.

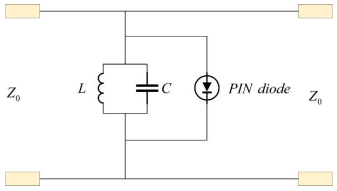

Figure 3. Equivalent Circuit Model of State-Switchable AFSS

Based on the aforementioned design concept, the proposed AASS structure is illustrated in Figure 4, where the yellow and blue regions represent the metallic layers and dielectric substrates, respectively. The overall structure consists of a double-layer ASS on the top and a single-layer AFSS at the bottom, cascaded with an air spacing of h_2 between them. The upper ASS is composed of two identical FSS layers separated by an air gap. Each layer consists of a cross-shaped slot loaded with meandered arms, arranged with a 90° rotational symmetry about the center. The spacing between the two ASS layers is denoted as h_1. The lower AFSS layer is formed by a square-loop slot structure, in which PIN diodes are symmetrically loaded around the slot to enable state switching. The dielectric substrates used for both the ASS and AFSS are made of F4B material with a relative permittivity of ε_r =2.65 and a loss tangent of $\tan\delta$ =0.0001, and all substrates have a uniform thickness of t.

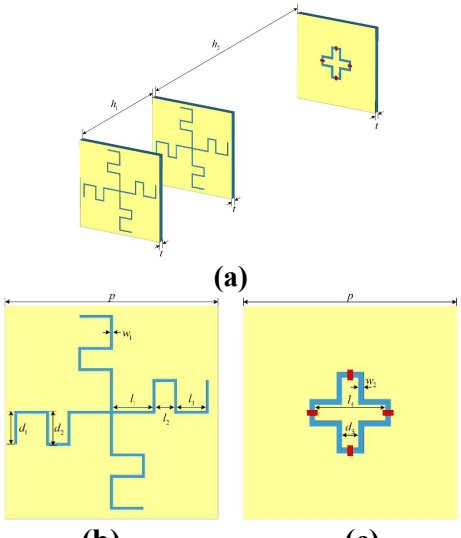

Figure 4. AASS Structural Diagram (a) 3-D View of the Whole Structure (b) Top View of the ASS Unit Cell (c) Top View of the AFSS Unit Cell (p =8mm, t=0.508mm, h_1 =12mm, h_2 =25mm, l_1=1.5mm, l_2=0.7mm, l_3=1.1mm, l_4=2.6mm, d_1 =1.25mm, d_2 =1.3mm, d_3 =0.6mm, w_1 =0.1mm, w_2 =0.2mm)

To further analyze the electromagnetic response of the proposed AASS, the overall ECM is presented in Figure 5. In this model, the parallel combination of L_1 and C_1 represents the first and second layers of meander-loaded cross-shaped slot structures. Similarly, the parallel combination of L_2 and C_2 corresponds to the third-layer square-loop slot structure. In addition, a switching branch connected in parallel is introduced to model the loaded PIN diodes, enabling state switching functionality. The transmission line impedances Z_t and Z_0 represent the dielectric substrates and the air spacing layers, respectively, where t, h_1, and h_2 denote the thickness of the dielectric substrate and the air gaps.

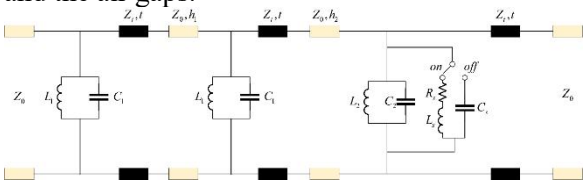

Figure 5. Overall Equivalent Circuit Model of AASS

The core of the proposed three-layer structure lies in the functional decoupling and coordinated design between the ASS and AFSS. The upper two ASS layers primarily determine the angular selectivity by establishing a transmission channel only at an incident angle of 60°, while the bottom AFSS layer controls the switching between transmission and reflection states, thereby regulating the overall electromagnetic response under the constraint of angular selectivity. Under the 60° incidence condition, the ASS layers provide a well-matched impedance environment, and the overall transmission performance is mainly governed by the AFSS layer. Specifically, when the AFSS operates in the transmission state, the entire structure exhibits high transmission; when it switches to the reflection state, the structure transitions to a shielding state. In contrast, under non-60° incidence conditions, the ASS layers introduce significant impedance mismatch. As a result, even if the AFSS is in the transmission state, the overall structure still exhibits strong reflection, thereby achieving dual selectivity in both angle and electromagnetic state.

3. Simulation Results

Full-wave simulations of the proposed AASS are carried out using CST Microwave Studio to further validate its electromagnetic response characteristics. As shown in Figure 6, when the PIN diodes are in the OFF state, the structure exhibits an excellent stopband response under TE polarization. As the incident angle increases from 0° to 89°, the transmission coefficient S21 remains below −25 dB at 11.75 GHz, indicating strong reflection of the incident electromagnetic waves. Under TM polarization, the transmission window is confined to the oblique incidence case of 60° at 11.75 GHz, corresponding to the blue region in the simulated response. At the remaining incident angles, the surface mainly shows a reflective state.

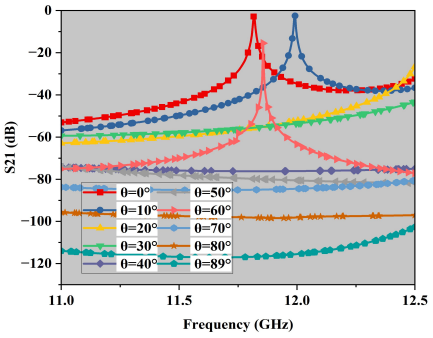

(a)

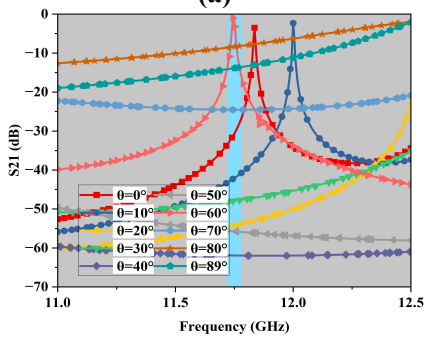

(b)

Figure 6. Transmission Coefficients Under (a) TE and (b) TM Polarization

Figure 7 shows the angular response at 11.75 GHz and gives a direct comparison among the simulated polarization-angle combinations. For TM incidence, transmission is retained only at 60°; the other cases, including the nonselected angles and polarization states, are suppressed by reflection.

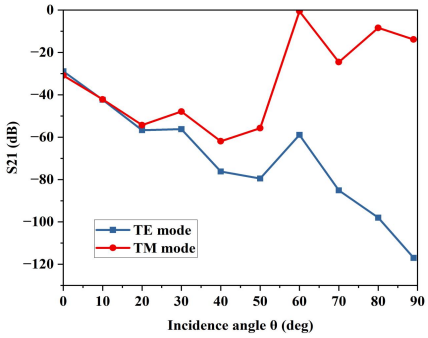

Figure 7. Simulation of Angle Selectivity in 11.75 GHz

The transmission behavior is therefore limited to obliquely incident TM-polarized waves. This selectivity is related to the polarization-dependent field distribution and the corresponding equivalent-circuit response. In the TM case, the electric field contains a normal component in the plane of incidence, which couples more effectively to the current paths in the unit cell and produces a stronger resonant response. In contrast, for TE polarization, the electric field orientation does not align with the dominant current paths of the structure, making it difficult to excite an effective resonance mode and resulting in an overall reflective response.

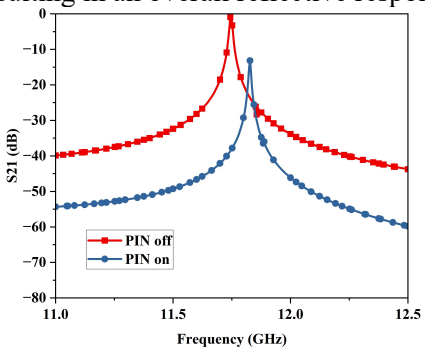

Figure 8. Transmission Coefficients of the AASS in Two Diode States

The results presented above correspond to the OFF state of the PIN diodes. The state-switching functionality of the proposed AASS is further verified in Figure 8. Under TM polarization with an incident angle of 60°, when the PIN diodes are switched to the ON state, the passband at 11.75 GHz is successfully transformed into a stopband, enabling the transition from transmission to reflection.

Compared with conventional ASS or FSS structures with single functionality, the proposed design offers significant advantages in terms of angular selectivity and reconfigurability. In addition, the relatively simple configuration ensures its feasibility for practical engineering implementation.

4. Conclusion

In this paper, a three-layer AASS is proposed. By cascading a double-layer ASS with a single-layer AFSS, the proposed structure achieves the integration of angular selectivity and dynamic control of electromagnetic response. Based on the equivalent impedance model and multilayer coupling mechanism, the underlying physical mechanism enabling highly selective transmission under specific incidence conditions is clarified. The results show that, at the operating frequency of 11.75 GHz, the proposed structure has high transmission only for TM-polarized waves with an incident angle of 60°, while reflecting strongly for other incident angles and polarizations, thus achieving good angular selectivity. Moreover, by adjusting the operating state of the AFSS layer, the transmission and shielding states can be effectively switched under the condition of 60° incidence, which allows the combination of angular selectivity and functional reconfigurability. The proposed design has promising application prospects in spatial electromagnetic filtering, directional communication, intelligent radomes and electromagnetic protection.

References

[1] Sheng X, Wang H, Liu N, et al. A conformal miniaturized bandpass frequency-selective surface with stable frequency response for radome applications. IEEE Transactions on Antennas and Propagation, 2024, 72(3): 2423-2433.

[2] Chen X, Tan J, Kang L, et al. Frequency selective surface toward 6G communication systems: A contemporary survey. IEEE Communications Surveys & Tutorials, 2024, 26(3): 1635-1675.

[3] Yang R, Luo Z, Liang J C, et al. Reconfigurable Metasurface with Multiple Functionalities of Frequency‐Selective Rasorber, Frequency‐Selective Surface, Absorber, and Reflector. Advanced Materials Technologies, 2025, 10(2): 2400966.

[4] Zheng W, Yang Y, Feng T X, et al. Systematic inverse design of miniaturized frequency selective surfaces based on microwave network theory and NSGA-III. IEEE Transactions on Microwave Theory and Techniques, 2025.

[5] Yun D J, Hwang I J, Jung H, et al. Multifunctional Radome-Based Frequency Selective Surface Composites for Stealth Applications. IEEE Antennas and Wireless Propagation Letters, 2025.

[6] Meng X, Lv M, Huang M, et al. Efficient modeling method for Quasi-Conical frequency selective surface radomes of aircraft. AEU-International Journal of Electronics and Communications, 2025: 155948.

[7] Idrees M, He Y, Wen Y, et al. Design of a Miniaturized and Polarization-Independent Frequency-Selective Surface for Targeted EMI Shielding. Applied Sciences, 2025, 15(8): 4534.
[8] Zhang L M, Ding X, Bozzi M. Heterogeneous reconfigurable frequency selective surface with ultrawide range performance. IEEE Transactions on Microwave Theory and Techniques, 2025.
[9] Li Y, Ma Y, Ren P, et al. Design of angle-selective surface with narrow-angle filtering for variable frequency. IEEE Antennas and Wireless Propagation Letters, 2025.
[10] Chen Z, Shen Z. Absorptive polarization-selective surface based on strip-line resonances. IEEE Antennas and Wireless Propagation Letters, 2024, 23(8): 2541-2545.
[11] Xu H, Zhou D, Liu Q, et al. Angle-Selective Surface Based on Frequency-Selective Surface Using Compact Double-Layer Patch-Coupled Resonance. IEEE Antennas and Wireless Propagation Letters, 2024, 24(1): 117-121.
[12] Kou N, Yu S. Angular selectivity based on odd mode resonance of frequency selective surface. IEEE Antennas and Wireless Propagation Letters, 2022, 21(11): 2151-2155.
[13] Chen Z, Du C, Liu J, et al. Design methodology of dual-polarized angle-selective surface based on three-layer frequency-selective surfaces. IEEE Transactions on Antennas and Propagation, 2023, 71(11): 8704-8713.
[14] Qian Q, Xu C, Wang C. All-dielectric polarization-independent optical angular filter. Scientific reports, 2017, 7(1): 16574.
[15] Guo J, Chen S, Jiang S. Optical broadband angular filters based on staggered photonic structures. Journal of Modern Optics, 2018, 65(8): 928-936.
[16] Mao X, Zhao Y, Hu X J, et al. Broadband Dual-Polarized Angle-Selective Surface Based on Multi-Layered Frequency-Selective Surfaces. IEEE Antennas and Wireless Propagation Letters, 2025.
[17] Hong Y, Shen Z. Dual-polarized bilayer angle-selective structure. IEEE Antennas and Wireless Propagation Letters, 2023, 23(2): 823-827.
[18] Zhang K, Du C, Cao Y, et al. Via-Free Dual-Polarized Angle-Selective Surface. IEEE Antennas and Wireless Propagation Letters, 2025.
[19] Xu R, Ren P, Li Y, et al. Analysis and Design of SIWC-Based AFSS With Polarization Selectivity and Three Independently Controllable Poles. IEEE Transactions on Microwave Theory and Techniques, 2025.
[20] Zhou H, Lu L, Ding J. A Design Method of Reconfigurable Frequency Selective Surface Based on Image Generation and Database Establishment. IET Microwaves, Antennas & Propagation, 2025, 19(1): e70067.
[21] Li Z, Weng X, Li Y, et al. Reconfigurable Active FSS with Switchable Passband/Stopband Response. IEEE Transactions on Antennas and Propagation, 2026.
[22] Wang Z, Zhang J, Hou J, et al. Wideband and wide-angle switchable spatial filter/shielding with polarization-independent response. IEEE Antennas and Wireless Propagation Letters, 2023, 22(6): 1421-1425.
[23] Li Y, Xu F, Gu C, et al. Design of Angle-Selective Surface With Narrow Angular Domain and Ultra-Narrow Angular Transition Range. IEEE Antennas and Wireless Propagation Letters, 2025

